Electron Loss Cross Sections for a Heavy Ion Beam Probe

M. NISHIURA, T. IDO, A. SHIMIZU, R.K. JANEV[1)], T. KATO, V.P. SHEVELKO[2)], S. KATO, K. TSUKADA, M. YOKOTA, H. OGAWA, T. INOUE, H. NAKANO, Y. HAMADA and LHD Experimental Group

National Institute for Fusion Science, National Institutes of Natural Sciences, 322-6 Oroshi, Toki, Gifu, 509-5292 Japan

[1)]*Macedonian Academy of Sciences and Arts, P.O. Box 428, 1000 Skopje, Macedonia*

[2)]*P.N. Lebedev Physical Institute, Leninskii prospect 53, 119991 Moscow, Russia*

(Received 6 December 2006 / Accepted 10 May 2007)

Electron loss cross sections of Au^+ and Au^{2+} by electron and proton impact are calculated by using respectively the Lotz formula and the LOSS and CAPTURE computer codes. The corresponding rate coefficients have also been calculated. Using this information, the signal levels of heavy ion beam probe in the Large Helical Device are estimated. The calculated beam currents at the detector position are compared with the detected beam currents in the MeV energy range for a plasma electron density of $1 \times 10^{19}\,\mathrm{m}^{-3}$ and electron temperature of 1.5 keV. The obtained cross section / rate coefficient data can also be used for reconstruction of electron density and temperature profiles.

Keywords: heavy ion beam probe, plasma potential, electric field, electron loss cross section, gold

DOI: 10.1585/pfr.2.S1099

1. Introduction

The heavy ion beam probe (HIBP) system is a reliable method for measuring the local plasma potential and fluctuations. The system has already been installed in the Large Helical Device (LHD) at NIFS. The accelerated Au^- beam undergoes double charge exchange and the resulting Au^+ beam (primary beam), whose energy normally reaches up to 6 MeV, is injected into the LHD plasma. The MeV Au^+ beam is ionized by plasma electrons and ions (undergoing also charge exchange with the latter), and the resulting Au^{2+} beam (secondary beam) is detected by an energy analyzer. The local plasma potential at the ionization position is obtained from the energy change between the injected beam and the detected one.

In the basic design phase of LHD-HIBP system, the ratios of primary beam current to secondary beam current are predicted by taking into account only the electron-impact ionization processes [1]. In absence of experimental cross sections, the Lotz formula [2] was used to determine the cross sections of Au^+ and Au^{2+} for electron impact ionization. Based on such estimates, the parameters of beam accelerator for injector and beam energy analyzer for detector were determined. In 2004, the HIBP system detected the secondary beam signal successfully during the ion cyclotron resonance heating discharge. The recent LHD experimental results, however, suggest that a diagnostics appropriate for high temperature (~10 keV) and high density (~$10^{20}\,\mathrm{m}^{-3}$) plasmas is required in order to study the plasma confinement and transport in LHD. Under such plasma conditions, it is expected that the role of charge exchange and ionization (i.e. electron loss) processes of Au^+ and Au^{2+} ions with the plasma protons could also be important in the calculations of beam attenuation in the plasma.

In the present paper we calculate the Au^+ and Au^{2+} beam stopping cross sections and the secondary beam signal at the detector by including the electron loss processes of these ions with both plasma electrons and protons. The experimental signal level of the secondary beam under typical experimental conditions is compared with the calculated signal.

author's e-mail: nishiura@nifs.ac.jp

2. Electron-Impact Ionization Processes

In absence of experimental cross section or calculations with more sophisticated theoretical methods for the electron-impact ionization processes

$$Au^{q+} + e \rightarrow Au^{(q+1)+} + 2e, \quad q = 1, 2 \qquad (1)$$

A reasonable and widely adopted approach to estimate the cross sections of these processes is to use the Lotz formula [2]

$$\sigma_{ei}(T_e) = 4.5 \times 10^{-14} \sum_{i=1}^{N} \xi_i \frac{\ln(E/I_i)}{E/I_i}, \quad [\mathrm{cm}^2] \qquad (2)$$

where E is the collision energy, I_i is the ionization potential of i-th electronic subshell, and ξ_i is the number of electrons in that subshell. The summation in Eq. (2) runs over all subshells. The ionization cross sections for Au^+ and Au^{2+}, calculated by the above formula, are shown in Fig. 1(a). We

Table 1 Parameters required in the Lotz formula for gold and copper [3].

Configuration	I_i(eV)	ξ_i
Au^{+}[Xe]4f^{14}5d^{10}	20.5	10
Au^{2+}[Xe]4f^{14}5d^{9}	30.0	9
Cu^{+}[Ar] 5d^{10}	20.29	10
Cu^{2+}[Ar]5d^{9}	36.83	9

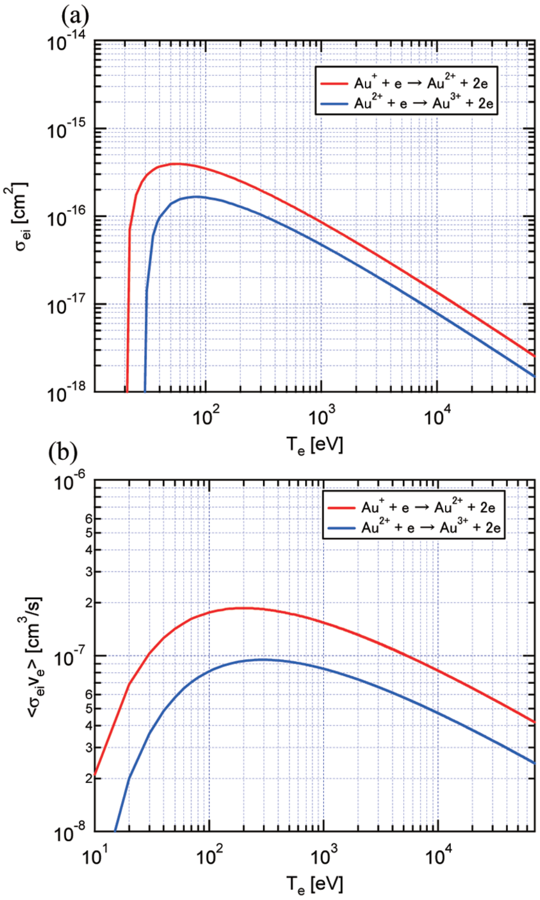

Fig. 1 (a) Ionization-cross sections of Au^{+} and Au^{2+} calculated by the Lotz formula. (b) Rate coefficients for the ionization of Au^{+} and Au^{2+} by electron impact.

note that the outer 5*d* subshell almost exclusively determines the cross sections in the entire energy region investigated. The parameters I_i and ξ_i are listed in Table 1. (The ionization potentials are taken from Ref. [3]). In Table 1, we also give the values of these parameters for copper, as one of the possible beam candidates for LHD-HIBP.

When calculating the ionization rate coefficient, we treat the 6 MeV Au^{+} ions as a mono-energetic (with velocity = 2.4×10^6 m/s) beam, passing through the plasma electrons having 1 keV temperature (thermal velocity ~ 2×10^7 m/s). Assuming a Maxwellian electron velocity distribution, the ionization rate coefficient, with the expression (2) for the cross section, can be obtained as

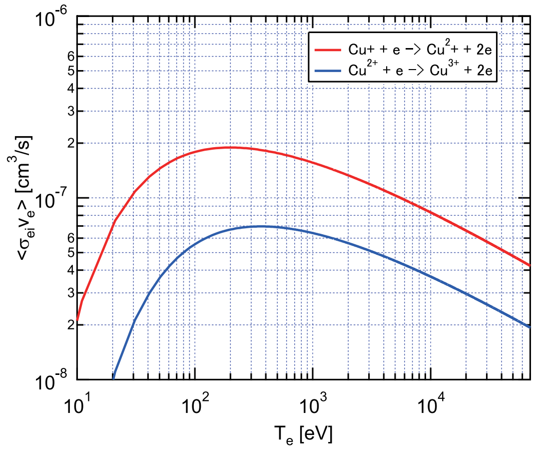

Fig. 2 Rate coefficients of Cu^{+} and Cu^{2+} by electron impact ionization using Eq. (3).

$$\langle \sigma_{ei}(T_e)\, v_e \rangle = 3.0 \times 10^{-6} \sum_{i=1}^{N} \frac{\xi_i}{T_e^{1/2} I_i} \times \int_{I_i/T_e}^{\infty} \frac{\exp(-x)}{x} dx, \quad (3)$$

where T_e is the electron temperature in eV, v_e is the electron velocity and $x = m_e v_e^2/(2T_e)$. The rates $\langle \sigma_{ei}^{1,2}(T_e) v_e \rangle$ for $Au^{+} \rightarrow Au^{2+}$ and $\langle \sigma_{ei}^{2,3}(T_e) v_e \rangle$ for $Au^{2+} \rightarrow Au^{3+}$ are plotted as a function of T_e in Fig. 1(b). The corresponding rate coefficients for copper are plotted in Fig. 2.

We should note that the cross section estimates by the Lotz formula can be uncertain within a factor of two, or so.

3. Ion Impact Charge Exchange and Ionization Processes

It is well known that at high collision energies (hundreds of keV/nucleon) the cross sections for proton impact inelastic processes are much higher than those with electrons. Moreover, some of these processes, e.g., charge exchange, have large cross sections even at low (few keV/nucleon) collision energies. Therefore, in the context of energetic Au^{q+} ion attenuation in the plasma it is necessary to consider also the impact proton processes that result in lost of one or more electrons from the beam ion. The simplest of these processes are the charge exchange and ionization of the beam ion on plasma protons, i.e.,

$$Au^{q+} + H^{+} \rightarrow Au^{(q+1)+} + H, \quad q = 1, 2 \quad (4)$$
$$\rightarrow Au^{(q+1)+} + H^{+} + e \quad (5)$$

The combined effect of these two processes is called electron loss. These processes have not been included in the beam attenuation analysis of HIBP diagnostics so far.

We have performed cross section calculations the electron loss cross section of Au^{+} on protons in a broad energy range by using the CAPTURE [4] and LOSS [5]

Table 2 Parameters used for the analytic fit function of electron loss cross sections for Au^+ and Au^{2+}.

A_1	A_2	A_3	A_4
4.64E6	3.49E6	1.00E4	1.06E-13
A_5	A_6	A_7	A_8
2.07E-6	-1.36	5.26E4	-2.50

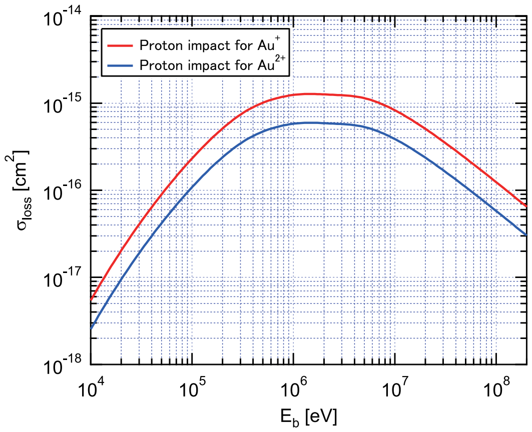

Fig. 3 Electron loss cross sections for Au^+ and Au^{2+} by proton impact.

computer codes, with inclusion the contributions from 5d, 5p, 5s, 4f and 4d subshells. As in the case of electron-impact ionization, the predominant contribution to the total electron loss cross section $\sigma^{1,2}_{loss}(E_b)$ comes from the 5d subshell. The electron loss cross section for the Au^{2+} + H^+ collision, $\sigma^{2,3}_{loss}(E_b)$, was estimated using $\sigma^{1,2}_{loss}(E_b)$ and the electron loss cross section scaling [6], giving $\sigma^{2,3}_{loss}(E_b) \approx 0.467\sigma^{1,2}_{loss}(E_b)$. E_b in these expressions is the beam energy. We note that the calculated $\sigma^{1,2}_{loss}(E_b)$ cross section at high energies agrees well with empirical scaling derived from the experimental proton – heavy ion ionization cross sections [7].

The electron loss cross sections for Au^+ can be represented by the analytic fit function

$$\sigma_{loss} = 10^{-16} A_1 \left[\frac{\exp(-A_2/E_b)\ln(1+A_3E_b)}{E_b} + \frac{A_4 \exp(-A_5E_b)}{E_b^{A_6} + A_7E_b^{A_8}} \right] \quad [\mathrm{cm}^2] \tag{6}$$

with the parameters A_i given in Table 2. The cross sections $\sigma^{1,2}_{loss}(E_b)$ and $\sigma^{2,3}_{loss}(E_b)$ are shown in Fig. 3.

For the typical condition of 6 MeV Au^+ beam and thermal proton temperature of T_i = 1 keV, for the rate coefficients of electron loss processes we can take the product of corresponding electron loss cross section and the beam velocity. The resulting rate coefficients are shown in Fig. 4. The rate coefficients of electron loss processes ($3\sim30\times10^{-8}$ cm^{-3}/s) are of the same order

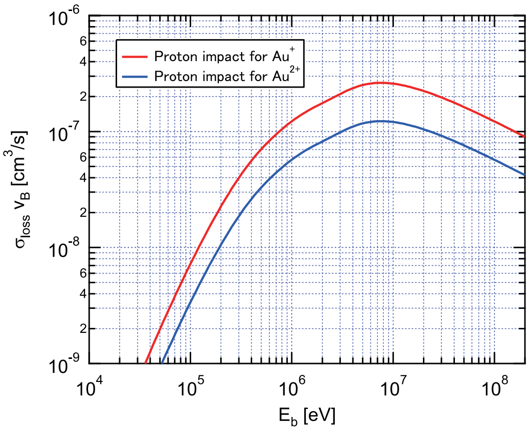

Fig. 4 Electron loss rate coefficients for Au^+ and Au^{2+} by proton impact.

of magnitude as those for electron impact ionization ($4\sim20\times10^{-8}$ cm^{-3}/s). With increasing the plasma temperature above 1 keV, however, the rate coefficient for electron impact ionization rapidly decreases and the importance of proton impact electron loss processes in beam attenuation increases.

4. Beam Attenuation Dynamics

The considerations in the previous sections indicate that the beam attenuation in plasmas should include both of electron- and ion- impact electron loss processes. The attenuation of beam density, n_B, per unit path length is given by

$$v_B \frac{dn_B}{dl} = -n_e n_B \left\langle \sigma^{1,2}_{ei} v_e \right\rangle - n_{H^+} n_B \left\langle \sigma^{1,2}_{loss} v_B \right\rangle, \tag{7}$$

where v_B is the beam velocity.

This rate equation is integrated over the path length l between the injected point $l_{in} = 0$ at the plasma boundary and the ionization (observation) point l_1. When the plasma electron temperature and density are assumed to be the uniform, the primary beam current at $l = l_1$ becomes

$$I_{B1} = I_{B0} \exp\left(-n_e \frac{\left\langle \sigma^{1,2}_{ei} v_e \right\rangle}{v_B} l_1 - n_{H^+} \frac{\left\langle \sigma^{1,2}_{loss} v_B \right\rangle}{v_B} l_1 \right). \tag{8}$$

where I_{B0} and I_{B1} are the primary beam currents at $l = 0$ and 1, respectively. The densities of electrons, protons, and gold ions are denoted by n_e, n_{H^+}, and n_B, respectively. The secondary ion beam current I_{B2} at the exit point $l = l_2$ from the plasma boundary is given by

$$I_{B2} = \frac{2\kappa_{mcp} I_{B1} \delta l}{v_B} \left(n_e \left\langle \sigma^{1,2}_{ei} v_e \right\rangle + n_{H^+} \left\langle \sigma^{1,2}_{loss} v_B \right\rangle \right) \times \exp\left(-n_e \frac{\left\langle \sigma^{2,3}_{ei} v_e \right\rangle}{v_B} l_2 - n_{H^+} \frac{\left\langle \sigma^{2,3}_{loss} v_B \right\rangle}{v_B} l_2 \right), \tag{9}$$

where the detection efficiency of the micro-channel plate $\kappa_{mcp} = 0.3$ is extrapolated from that in the lower energy region of the datasheet and δl is the effective observation length.

Substituting Eq. (8) into Eq. (9), the ratio $(I_{B2}/I_{B0})_{\rm cal}$ is calculated using the effective observation length δl = 0.6 mm, and $l_1 = l_2 = 1$ m. We have found that the ion-ion collision processes reduce the ratio $(I_{B2}/I_{B0})_{\rm cal}$, and calculated signals become closer to experimental ones. Still the disagreement between calculated and measured signals remains large. For the plasma with $n_e = 1 \times 10^{19}\,{\rm m}^{-3}$ and $T_e = 1.5$ keV, and beam energies of 1.62 MeV and 5.33 MeV, for the ratio $\chi \equiv (I_{B2}/I_{B0})_{\rm exp} / (I_{B2}/I_{B0})_{\rm cal}$ we obtain the values 8.7×10^{-3} and 5.4×10^{-3}, respectively. There could be several reasons for this significant disagreement between experimental and calculated signals. The attenuation kinetics described above includes only the simplest electron loss processes. Electron and proton impact excitation-autoionization processes may significantly increase the total ionization cross section. The electron loss by plasma impurities, which is proportional to the impurity ionic charge, may also significantly contribute to the beam stopping cross section. Multi-step processes, such as excitation followed by electron loss (ionization or charge exchange) are another possible contributor to the beam stopping cross section. Residual neutrals, especially at the plasma periphery, having large charge exchange cross sections with the Au^{q+} ions, can also significantly contribute to the beam loss. Presence of a metastable fraction in the primary or secondary beam can significantly increase the electron loss cross sections for the corresponding ion. Finally, the assumption about the constant plasma parameters along the ion beam paths certainly affects the calculated signal. Furthermore, uncertainties in the beam path length will have a dramatic (exponential) effect on the signal intensity. We should also mention that an experimental uncertainty still exists regarding the detection efficiency of the multi-channel plate. A serious further effort is needed for resolving these issues.

Acknowledgments

One of the authors (M. N.) would like to thank Dr. Fujisawa of NIFS for useful discussions. This work was supported by NIFS06ULBB505, NIFS06KCBR001, JSPS Grant Wakate-B No.18740357, and NIFS/NINS under the project of Formation of International Network for Scientific Collaborations.

[1] A. Fujisawa *et al.*, IEEE Trans. Plasma Sci. **22**, No.4, 395 (1994).
[2] W. Lotz, Astrophys. J. Suppl. **14**, 207 (1967).
[3] C.W. Allen, *Astrophysical Quantities*, 3rd ed. (Athlone Press, 1973).
[4] V.P. Shevelko, O. Rozmey, H. Tawara *et al.*, J. Phys. B **37**, 201 (2004).
[5] V.P. Shevelko, I. Yu. Tolstikhina and Th. Stoehler, NIMB Phys. Res. B **184**, 295 (2001).
[6] R.K. Janev, Phys. Rev. A **28**, 1810 (1983).
[7] M.F. Watts, C.J. Hopkins, G.C. Angel *et al.*, J. Phys. B **19**, 3739 (1986).